

The Mathematics of Fuel-to-Distance-Optimal Flight

Robert Schaback¹

Draft of April 15, 2017

Abstract: Within the standard framework of quasi-steady flight, this paper derives a speed that realizes the minimal fuel consumption per nautical mile. If this speed is chosen at each instant of a flight plan $h(x)$ giving altitude h as a function of distance x , a variational problem for finding an optimal $h(x)$ can be formulated and solved. It yields optimal fuel-to-distance flight plans, and these turn out to consist of mainly three phases using the optimal speed: starting with a climb at maximal continuous admissible thrust, ending with a continuous descent at idle thrust, and in between with a transition based on a solution of the Euler-Lagrange equation for the variational problem. This will use less fuel in total than the competing optimal lift-to-drag or *green dot* or optimal fuel-to time speed assignment and the flight will arrive earlier at the destination, due to higher ground speed. A similar variational problem is derived and solved for speed-restricted flights, e.g. below 10000 ft. Various numerical examples based on a Standard Business Jet are added for illustration. There, the fuel savings range between 14% in cruise and 50% in climb when compared to green dot speed proposed by Airbus.

1 Introduction

The problem of calculating flight trajectories that minimize fuel consumption has a long history, see e.g. the references in [2, 12, 15]. Various mathematical techniques were applied, ranging from parametrizations of trajectories [2, 15] via certain forms of Optimal Control Theory [3, 5, 10] to Multiobjective Optimization using various cost functionals [9, 6, 13].

This paper takes a quite simple approach based on the equations of quasi-steady flight, staying close to basic classroom texts [7, 11] and focusing on standard numerical methods that just solve systems of ordinary differential equations. There is no constraint on fixed altitude, but wind effects and fixed arrival times are ignored [4, 3], and the only objective is fuel savings over the full flight distance.

¹Prof. Dr. R. Schaback

Institut für Numerische und Angewandte Mathematik,
Lotzestraße 16-18, D-37083 Göttingen, Germany
schaback@math.uni-goettingen.de
<http://www.num.math.uni-goettingen.de/schaback/>

Of course, this can only be done by additional ingredients that allow to determine the variables that usually require control, e.g. thrust T , flight path angle γ , speed V , or lift L , whichever are chosen. We give a summary of the mathematical argument now, focusing on its practical consequences, delaying technical machinery to the core of the paper.

Starting with quasi-steady flight in Section 2, the standard differential equations for V and γ turn into algebraic equations, and we use one for determining lift in terms of the other variables, and the other for an equation connecting the thrust-to-weight ratio T/W to γ , V , and altitude h in a specific way, given the drag polar. The next step in Section 3 is to rewrite the quasi-steady flight equations for h , T , W and distance x in terms of x instead of time, and to minimize the total fuel consumption over the full flight distance, i.e. the x -integral over $-dW/dx$. Inserting the equation for T/W based on quasi-steady flight, the integrand can be minimized as a function of speed at each instance of the flight. For horizontal flight, the resulting *fuel-to-distance-optimal* speed V_{FIX} turns out to be $\sqrt[4]{3}V_{LID} \approx 1.32V_{LID}$ compared to the *lift-to-drag-optimal* speed V_{LID} called *green dot* speed by Airbus, “*the recommended speed with the best climb performance, and the minimum fuel consumption*” [1, p. 943, 1240, 1276]. The latter uses about 14% more fuel than the V_{FIX} speed in level flight, but savings by V_{FIX} speed turn out later to be even larger in climb.

If V_{FIX} speed is used on a flight plan given as a function $h(x)$, this speed assignment, if it does not violate thrust or speed constraints, is fuel-to-distance optimal under all other choices of speed. But Section 4 goes one step further and varies the flight plans that allow V_{FIX} speed to calculate an optimal flight plan. Using V_{FIX} speed, the equation for quasi-steady flight now connects T/W with h and $h' = \tan \gamma$ only, because V_{FIX} speed now is a function of the other variables. Inserting this into the differential equation for $W(x)$ allows a transition to a differential equation for $\sqrt{W(x)}$ that does not contain W on the right-hand side anymore. Therefore, a minimum of $\sqrt{W(x_{start})} - \sqrt{W(x_{end})}$ can be written as an integral containing h and h' only. This is a standard case of the Calculus of Variations, allowing to calculate fuel-over-distance-optimal flight trajectories by solving the second-order Euler-Lagrange differential equation for that variational problem.

However, the solutions are implicitly constrained, mainly by the available thrust. By Calculus of Variations, solutions of restricted problems have to follow the constraints they tend to violate, and therefore Section 4 shows that optimal trajectories have three phases (see Figures 1 3, and 4):

- they start with a climb at maximal admissible continuous thrust at V_{FIX} speed,

- they end with *Continuous Descent* using idle thrust and V_{FIX} speed, but
- in between there is a short transition trajectory satisfying the Euler-Lagrange equation, flown at V_{FIX} speed as well. In this section, thrust is reduced continuously from full to idle in a specific way.

Section 5 explains how to calculate the restricted parts of the optimal trajectories, and it also considers horizontal flight under V_{FIX} speed, if required by Air Traffic Control (ATC).

So far, this suffices to treat fuel-optimal flight at altitudes above 10000 ft, but Section 6 also treats the standard restriction to 250 knots indicated airspeed (KIAS) below 10000 ft. The previous logic is not applicable, because a minimization over speed is not admitted anymore. Instead, the choice of the flight path angle is optimized now, and a second variational problem is derived to handle the speed restriction as a second constrained variational problem. A flight that climbs to horizontal flight at a prescribed altitude with 250 KIAS and fuel-to-distance-optimal angle adjustment will have two phases (see Figure 6):

- a climb at maximal admissible continuous thrust, and
- a short transition trajectory satisfying the Euler-Lagrange equation of the speed-restricted second variational problem. This section reduces thrust continuously from full to the amount necessary for V_{FIX} speed for level flight at the target altitude.

However, this is not fully satisfactory, because the V_{FIX} speed required to start the optimal trajectories in both cases is comparably high. This calls for two additional *acceleration phases*:

- one at *acceleration altitude* after reaching *clean configuration* to start the aforementioned fuel-optimal climb at 250 KIAS, and
- one at 10000 ft to link the two fuel optimal V_{FIX} trajectories outlined above.

Section 7 shows how to deal with this mathematically, and Section 8 provides examples showing that the additional accelerations for V_{FIX} pay off against the V_{LID} speed assignment. The latter uses less fuel per hour, but V_{FIX} needs less fuel per nautical mile and arrives earlier at the target altitude and speed, see Figure 10. The fuel savings in climb can reach 50%, mainly because the V_{FIX} climb uses a smaller climb angle and a higher speed.

Since all of this ignores restrictions by Air Traffic Control, Section 9 deals with flight level changes between level flight sections at V_{FIX} speed. All trajectory patches derived so far are combined by the final Section 10.

The mathematical procedures to calculate optimal fuel-to-distance trajectories are simple enough to be carried out rather quickly by any reasonably fast and suitably programmed Flight Management System, and the fuel-to-distance optimal speed V_{FlX} could be displayed on any Electronic Flight Instrument System.

All model calculations were done for the Standard Business Jet (SBJ) of [7] for convenience, using the simple turbojet propulsion model presented there. Symbolic formula manipulations, e.g. for setting up the Euler equations for the two variational problems, were done by MAPLE[©], and MATLAB[©] was used for all numerical calculations, mainly ODE solving. Programs are available from the author on request.

2 Quasi-Steady Flight

The standard [7, 11, 14] equations of *quasi-steady flight* are

$$\begin{aligned}\dot{x} &= V \cos \gamma \\ \dot{h} &= V \sin \gamma \\ \dot{W} &= -CT \\ 0 &= T - D - W \sin \gamma \\ 0 &= L - W \cos \gamma.\end{aligned}\tag{1}$$

with *distance* x , *altitude* h , *true airspeed* V , *flight path angle* γ , *specific fuel consumption* C , *weight* W , *thrust* T , *drag* D , and *lift* L . Like weight, lift, and drag, we consider thrust as a force, not a mass. Furthermore, we omit the influence of flaps, spoilers, or extended gears, i.e. we exclusively work in *clean configuration*. The equations live on short time intervals where speed V and angle γ are considered to be constant, but they will lead to useful equations that describe long-term changes of V and γ .

Lift and *Drag* are

$$L = \frac{1}{2}C_L\rho V^2S, \quad D = \frac{1}{2}C_D\rho V^2S$$

with the *air density* ρ , the *wing planform area* S , and the specific lift and drag coefficients C_L and C_D . Combining them with the *drag polar*

$$C_D = C_{D_0} + KC_L^2,$$

the two last equations of (1) imply

$$\begin{aligned}C_L &= \frac{2W \cos \gamma}{S \rho V^2} \\ T &= \frac{1}{2}C_{D_0}\rho V^2S + K\frac{2W^2 \cos^2 \gamma}{S \rho V^2} + W \sin \gamma.\end{aligned}\tag{2}$$

The *induced drag factor* K and the *lift-independent drag coefficient* C_{D_0} are dependent on Mach number, but we ignore this fact for simplicity. When it comes to calculations, and if speed and altitude are known, one can insert the Mach-dependent values whenever necessary, but we did not implement this feature and completely ignore the minor dependence on Reynolds number and viscosity.

For convenience, we also introduce

$$R := \frac{1}{2}\rho V^2 \frac{S}{W} = \frac{\frac{1}{2}\rho V^2}{\frac{W}{S}}$$

as the ratio between *dynamic pressure* $\frac{1}{2}\rho V^2$ and *wing pressure* W/S and call it the *pressure ratio*. Avoiding mass notions, we prefer *wing pressure* over the usual *wing loading*. It will turn out that the pressure ratio R is of central importance when dealing with quasi-steady flight. It combines speed, altitude (via ρ), weight, and wing planform area into a very useful dimensionless quantity that should get more attention by standard texts on Flight Mechanics. Examples will follow.

Using it, (2) simplifies to the dimensionless equation

$$\frac{T}{W} = C_{D_0}R + \frac{K \cos^2 \gamma}{R} + \sin \gamma \quad (3)$$

that governs quasi-steady flight. For a given thrust-to-weight ratio T/W , it describes the pilot's choice between speed (coded nicely into R hiding dependence on weight and altitude) and flight path angle. It depends on the drag polar, but is independent of propulsion properties.

The unique minimum of T/W over varying R is attained at

$$R_{LtD} = \sqrt{\frac{K}{C_{D_0}}} \cos \gamma = \frac{1}{2}\rho V_{LtD}^2 \frac{S}{W}, \quad V_{LtD}^2 = \frac{2W}{\rho S} \sqrt{\frac{K}{C_{D_0}}} \cos \gamma.$$

Going back to (2), it is easy to see that this realizes the well-known optimal *lift-to-drag* speed V_{LtD} in case of $\gamma = 0$, and therefore we use the suffix *LtD* for lift-to-drag optimality also in case of nonzero γ . Second, by (1), a minimal thrust for momentarily constant weight realizes a momentarily minimal fuel consumption over time, and this is why *LtD* speed implies minimal fuel consumption over time. Third, if we minimize γ as a function of R in (3) for fixed T/W , it turns out after some calculations that the maximal obtainable angle is assumed for V_{LtD} speed. Thus V_{LtD} coincides with the *green dot speed* used by Airbus: “*The recommended*

speed with the best climb performance, and the minimum fuel consumption" [1, p. 943, 1240, 1276]. But we shall see that using *LtD* speed makes flights take a seriously longer time than flights using *FtX* speed, and then the time-optimal fuel consumption is inferior to the distance-optimal fuel consumption that we study in the next section. *LtD* speed is more appropriate for situations with low thrust, e.g. engine-out situations, or for maximum endurance scenarios.

Since the *LtD* speed minimizes T/W , we remark that the inequality

$$\frac{T}{W} - \sin \gamma \geq 2\sqrt{KC_{D_0}} \cos \gamma$$

holds for quasi-steady flight in general, and equality is attained in the *LtD* situation. This relates necessary propulsion to the drag polar parameters and the required climb angle of an aircraft.

3 Fuel-to-Distance Optimal Speed

But the minimal fuel consumption at each instant of time will not necessarily produce the minimal fuel consumption over the flight distance. We replace time by distance derivatives, using primes instead of dots, and get

$$\begin{aligned} h' &= \frac{\dot{h}}{\dot{x}} = \tan \gamma, \\ W' &= \frac{\dot{W}}{\dot{x}} = \frac{-CT}{V \cos \gamma}, \end{aligned} \quad (4)$$

the remaining equations being invariant. We now assume that the specific fuel consumption C is independent of speed, and then the x -integral over the quantity

$$-\frac{W'(x)}{C} = \frac{1}{2} \frac{C_{D_0} \rho V S}{\cos \gamma} + K \frac{2W^2 \cos \gamma}{S \rho V^3} + W \frac{\tan \gamma}{V} \quad (5)$$

is to be minimized. We minimize the integrand over V to get a minimum at

$$\begin{aligned} R_{FtX} &= \frac{1}{2} \frac{\rho V_{FtX}^2 S}{W} = \frac{\sin \gamma}{2C_{D_0}} + \frac{1}{2C_{D_0}} \sqrt{\sin^2 \gamma + 12C_{D_0} K \cos^2 \gamma} =: A^2(\gamma), \\ V_{FtX}^2 &= \frac{2W}{\rho S} A^2(\gamma) \end{aligned} \quad (6)$$

after some elementary calculations. This determines a *fuel-to-distance optimal speed* V_{FtX} , if it does not violate external restrictions while minimizing over V . If it does, we take the extremal admissible value, because the minimum is unique.

Mimicking the “green dot speed” of Airbus and “BlueTEC” of Mercedes-Benz, one could call this “blue dot speed”, and it could be displayed on the EFIS alongside with green dot speed.

For horizontal flight, we get

$$R_{FtX} = A^2(0) = \sqrt{\frac{3K}{C_{D_0}}} = \sqrt{3}R_{LtD}, \quad V_{FtX} = \sqrt[4]{3} V_{LtD} \approx 1.32 V_{LtD}, \quad (7)$$

both speeds varying with altitude and weight for fixed R . Surprisingly, R_{FtX} , R_{LtD} and the corresponding ratios T/W for level flight are independent of altitude and depend only on the drag polar, not on propulsion characteristics. Since the available thrust decreases exponentially with altitude and weight decreases roughly linearly during cruise flight, the speeds V_{FtX} and V_{LtD} for level flight will both increase exponentially with altitude, but decrease with the weight loss. Consequently, a level flight at constant speed is never fuel-optimal, neither with respect to time (LtD) nor distance (FtX). The optimal strategy is to use FtX speed and let the square of it decrease with the weight. We provide more details in Section 5. In addition, FtX speed will be faster than LtD speed, and the flight will reach the target earlier. Compared to fuel usage in automobiles, we have a paradoxical situation for flights: *If you want to save fuel, use more power and go faster*, and we shall see more instances of this later.

By elementary calculations based on (6) we get

$$\left(\frac{T}{W}\right)_{FtX} = \frac{2}{\sqrt{3}} \left(\frac{T}{W}\right)_{LtD} \approx 1.15 \left(\frac{T}{W}\right)_{LtD}$$

and distance-relative fuel consumption using (4) is

$$\left(\frac{-W'}{C}\right)_{LtD} = \frac{\sqrt{3}\sqrt[4]{3}}{2} \left(\frac{-W'}{C}\right)_{LtD} \approx 1.1395 \left(\frac{-W'}{C}\right)_{FtX}$$

showing that for level flight the T/W ratio for FtX speed is 15% higher, due to a 32% higher speed, but the per distance fuel savings is roughly 14%. This results from V being in the denominator of (4).

For increasing flight path angle γ , these ratios increase roughly linearly with γ , making the savings even larger for steep climbs, but also R_{FtX} and V_{FtX} will increase. Thus one can expect very good fuel savings for steep climbs, but this requires a high initial speed. All of this is the motivation for taking a closer look at FtX speed in what follows.

Given the weight W , the necessary thrust for FtX speed is

$$T_{FtX} = W \tau_{FtX}(\gamma) \text{ with } \tau_{FtX}(\gamma) := C_{D_0} A^2(\gamma) + K \frac{\cos^2 \gamma}{A^2(\gamma)} + \sin \gamma \quad (8)$$

as a function of the flight path angle γ . Note that the connection depends only on the drag polar, not on propulsion. The LtD speed has a similar connection, namely

$$\frac{T}{W} = \sin \gamma + 2\sqrt{KC_{D_0}} \cos \gamma =: \tau_{LtD}(\gamma).$$

By inverting the monotonic function τ_{FtX} , one can calculate the resulting flight path angle γ for each given thrust, if FtX speed is to be flown, and similarly for LtD speed. This inversion is easy to do, the standard way or in symbolic calculation, e.g. using MAPLE[©].

4 Variational Problem

So far, we have determined the fuel-to-distance-optimal speed assignment for an arbitrary flight plan given as a function $h(x)$. If this V_{FtX} speed does not violate restrictions, it is the best one for that flight plan. But now we go a step further and vary the flight plans to find an optimal flight plan under all plans that allow the V_{FtX} speed assignment.

To this end, we insert V_{FtX} speed into the integral for the total fuel consumption to get a variational problem for the flight path $h(x)$. The integrand is

$$\begin{aligned} -W'(x) &= \frac{CT_{FtX}}{V_{FtX} \cos \gamma} \\ &= \sqrt{W(x)} \frac{\tau_{FtX}(\gamma)}{A(\gamma) \cos \gamma} C(h(x)) \sqrt{\frac{\rho(h(x))S}{2}} \end{aligned}$$

where we now made the dependence on x , h and $\gamma = \arctan h'(x)$ explicit. Recall that we already assumed the specific fuel consumption C to be independent of speed, but it usually will depend on altitude.

The substitution $Z(x) := \sqrt{W(x)}$ yields

$$-2Z'(x) = C(h(x)) \tau_{FtX}(\arctan h'(x)) \sqrt{\frac{\rho(h(x))S}{2}} \frac{\sqrt{1+h'(x)^2}}{A(\arctan h'(x))}$$

and eliminates W and Z from the right-hand side. Since it does not matter whether we reduce $W(x)$ optimally or $\sqrt{W(x)}$ optimally, we now minimize

$$\int_{x_0}^{x_1} C(h(x)) \sqrt{\frac{\rho(h(x))S}{2}} \tau_{FlX}(\arctan h'(x)) \frac{\sqrt{1+h'(x)^2}}{A(\arctan h'(x))} dx \quad (9)$$

to find an optimal flight plan under all flight plans with fuel-to-distance-optimal speed assignments. This is a classical variational problem, leading to a second-order Euler-Lagrange ODE for $h(x)$ by standard arguments.

The integrand is a product of a function F of h and a function G of h' . The latter is dependent only on the drag polar, not on propulsion, and derivatives wrt. h' can be generated by symbolic computation, e.g. using MAPLE[®]. The first part is $C(h)\sqrt{\rho(h)}$ up to constants and depends on propulsion only via the altitude-dependency of the specific fuel consumption $C(h)$. In simple models [7] for turbofans and turbojets, $C(h)$ is an exponential function of h , as well as the air density $\rho(h)$. Then symbolic computation will work as well for the h -dependent part.

A closer inspection of the Euler-Lagrange equation

$$h'' = \frac{G(h')}{G'(h')} \frac{F'(h)}{F(h)} - \frac{G'(h')}{G''(h')} h'$$

for the variational problem shows that $F'(h)/F(h)$ is a constant if $C(h)$ and $\rho(h)$ have an exponential law, and then the right-hand-side of the Euler-Lagrange equation is a pure equation in h' . Since the equation is also autonomous, the solutions $h(x)$ in the (x, h) plane can be shifted right-left and up-down, and they can be calculated by solving the above second-order differential equation.

Figure 1 shows typical solutions of the Euler-Lagrange equation for the Standard Business Jet (SBJ) model from [7], but the trajectories contain red parts where thrust is too high and green parts where thrust is below idle. A closer inspection of the differential equation reveals that the solutions are always concave in the (x, h) plane, and the speed is always decreasing.

This looks disappointing at first sight, but we have to take the thrust limits into account and view the variational problem as a *constrained* one. Such problems have the property that solutions either follow the Euler-Lagrange equation or a boundary defined by the restrictions.

We now visualize this in phase space, where we replace h' by $\gamma = \arctan h'$ for convenience. Figure 2 plots Euler-Lagrange trajectories $(h(x), \gamma(x))$ in (h, γ) phase

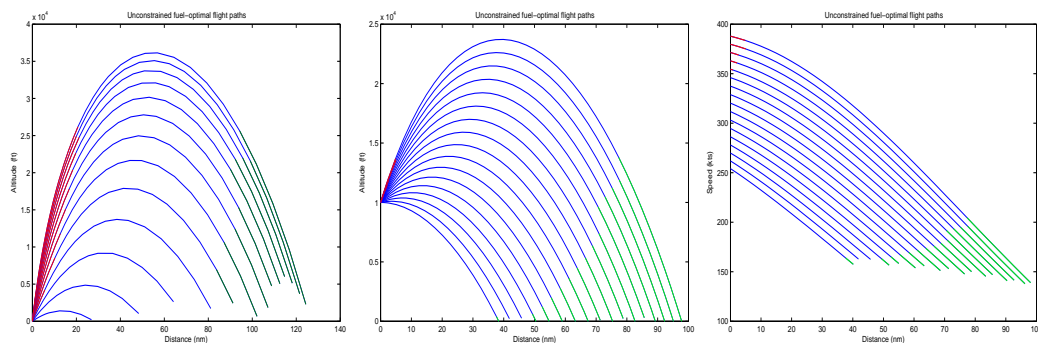


Figure 1: Some unconstrained flight paths: long distance, short distance, and speed profile for the SBJ model in [7]

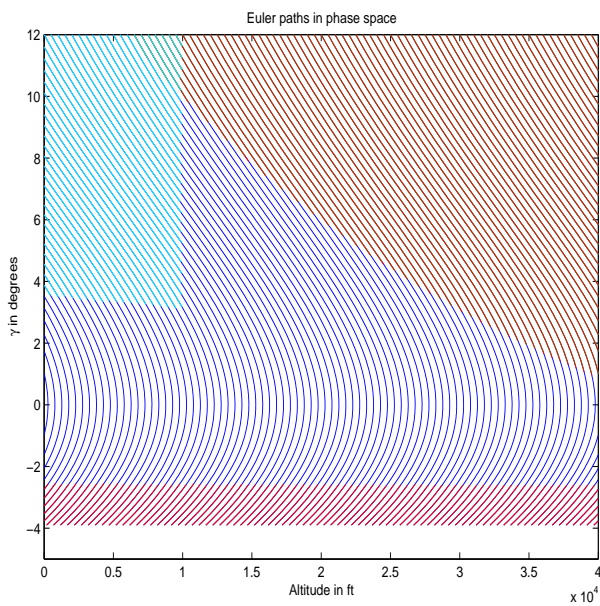


Figure 2: Euler-Lagrange flight paths going downwards through phase space

space, and marks the thrust-restricted areas in red, while the 250 KIAS (knots indicated airspeed) limit below 10000 ft is given in cyan. Since an explicit speed restriction is not compatible with our variation of V for getting an optimal speed, we have to ignore that area, but we shall come back to it in Section 6.

By the standard theory of constrained variational problems we now can read off the fuel-optimal flight paths above 10000 ft. If they do not hit the upper thrust limit in phase space, they are blue curves with a maximum altitude and going down in phase space until they reach the idle thrust boundary below. Compare with the plots of Figure 1 in (x, h) space. From the idle thrust boundary, they follow idle thrust and perform a continuous descent, moving to the left in phase space. If a flight path hits the upper thrust limit somewhere, it has to reach that point left-to-right in phase space, i.e. moving along the upper red/blue boundary to the right in phase space, until it leaves the boundary and then works as in the other case, going down along a blue solution of the Euler-Lagrange equation and ending up with continuous descent at idle thrust, going left in phase space.

This means that long-distance flights above 10000 ft that maintain FtX speed have necessarily three sections:

1. a climb/cruise at maximal continuous admissible thrust, proceeding in phase space from left to right along the upper red/blue boundary,
2. a transition following a solution of the Euler-Lagrange equation, downward along a blue curve in phase space,
3. and a continuous descent at idle thrust, along the lower red/blue boundary, going from right to left.

See the top plots in Figure 4 for other examples, in (x, h) space and (h, γ) phase space. We shall see later that all blue curves in the phase space figure arise in optimal flight plans, also for lower altitudes, as shown by Figure 12.

For the model aircraft in [7], Figure 3 shows a typical case. The flight is over 700 nm distance, starting at altitude 10000 ft, using a power setting $P = 0.97$ for the climb/cruise, and ending at 3000 ft. The figure shows the flight path, a close-up of the transition, speed, thrust, weight, and γ as functions of the distance. The transition piece takes about 13 nm and 2 minutes at roughly 400 kts, decreasing speed by roughly 50 kts and altitude by roughly 1500 ft. Flying the “bang-bang” trajectory above the transition piece at FtX speed is physically impossible due to the speed discontinuity, but a closer inspection confirms that it uses slightly more fuel than the transition piece satisfying the Euler-Lagrange equation.

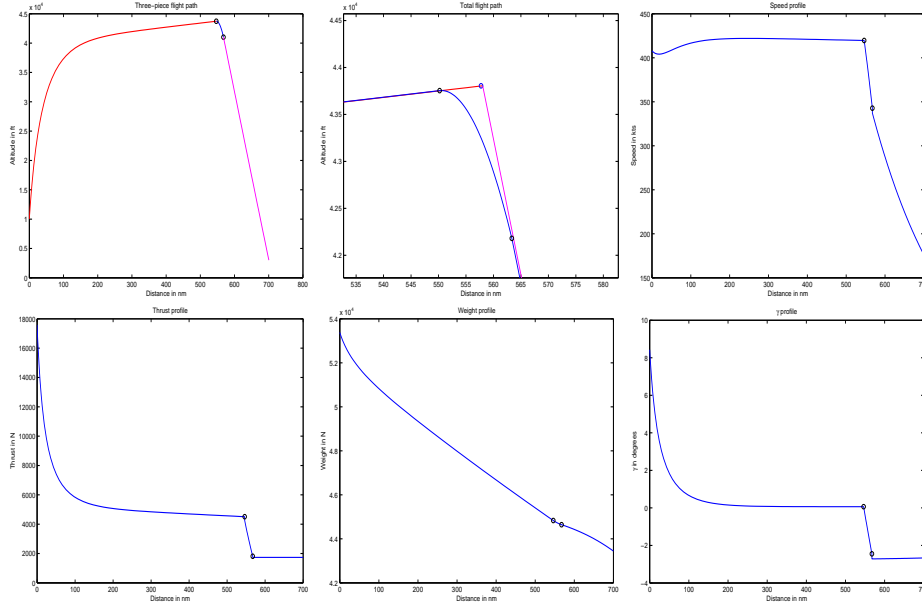


Figure 3: A three section flight over 700 nm with fuel-optimal speed. Flight path, close-up, speed, thrust, weight, and γ .

If we vary the point at which the second piece begins, we get Figure 4 that shows flights that either end at 3000 ft altitude or at empty fuel. Compare the phase space plot with Figure 2. The lower magenta line in the phase space plot must be thick because the flights arrive at idle thrust with different weights, and the continuous descent angle for V_{FIX} speed depends slightly on weight. The phase space plot 2 is for a single weight.

5 Prescribed Thrust or Altitude

To follow the thrust-restricted red/blue boundaries in Figure 2 in (h, γ) phase space, we assume thrust being given as a function of altitude, either as maximal admissible continuous thrust or idle thrust. The function τ_{FIX} of (8), being dependent only on the drag polar and nearly linear, is inverted symbolically and its inverse allows to calculate γ as a function of thrust and weight, using

$$\gamma(x) = \tau_{FIX}^{-1}(T(h(x))/W(x)), R_{FIX}(x) = A^2(\gamma(x)), V_{FIX}(x)^2 = \frac{2W(x)R_{FIX}(x)}{S\rho(h(x))}$$

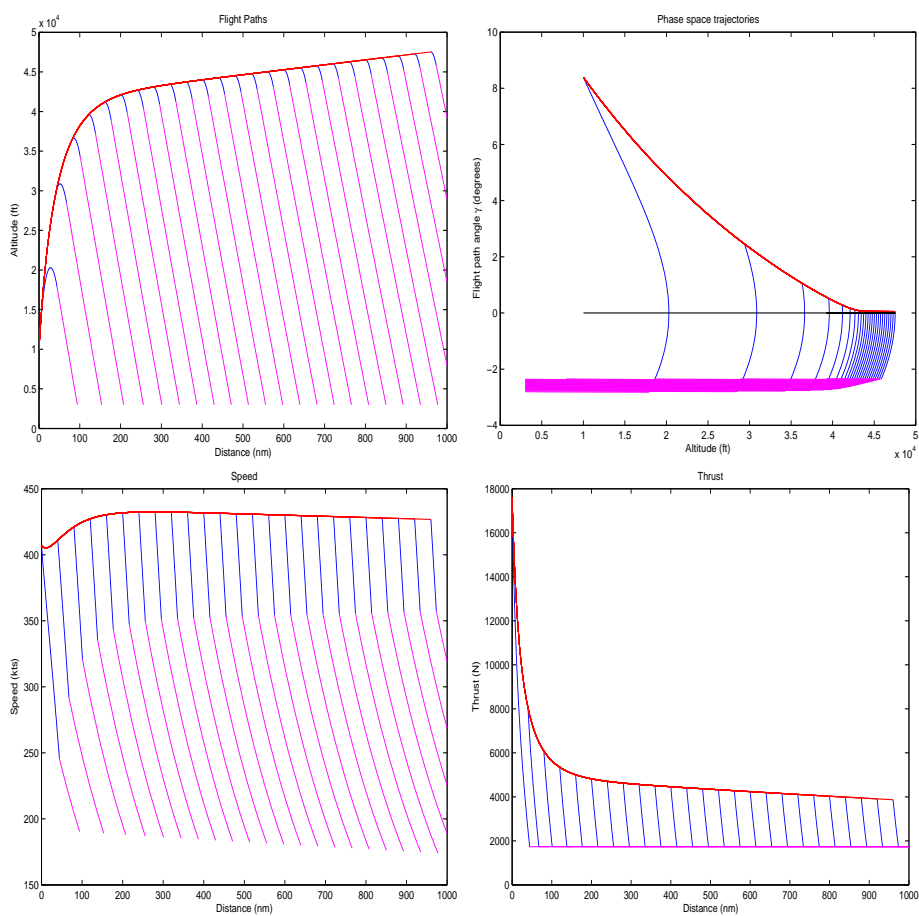


Figure 4: Three section flights with fuel-optimal speed. Flight paths, phase space trajectories, speed and thrust.

thus implementing FtX speed via (6). This is enough to set up an ODE system in terms of h and W as functions of x , namely

$$\begin{aligned} h'(x) &= \tan \gamma(x) \\ W'(x) &= -\frac{C(h(x))T(h(x))}{V(x) \cos \gamma(x)} \end{aligned}$$

using the above formulae. The trajectories in the previous figures were obtained that way.

Similarly, continuous descent at idle thrust with speed V_{FtX} is modelled. It is very close to, but not identical to using LtD speed, because the functions τ_{LtD}^{-1} and τ_{FtX}^{-1} are slightly different at small arguments like T_{idle}/W .

A flight at FtX speed at fixed altitude is just a point in (h, γ) phase space, but the associated flight will have a varying speed. We already know that the optimal FtX speed must decrease with weight, and it is easy to set up and solve the ODE in W for that, using (4), (6), (7), and (8). For the SBJ model of [7], Figure 5 shows the speed at altitudes from 40000 ft down in steps of 2000 ft as functions of the distance, and the reachable distance in nm as a function of altitude. The curves at the left-hand side start at full weight and stop when fuel is empty. They never reach stall speed, because they start at full fuel at sufficiently high values of the fuel-to-distance optimal speed, and the aircraft runs out of fuel before reaching stall speed. Summarizing, the speed reduction during a flight at constant altitude and optimal FtX speed is tolerably low.

6 Prescribed Speed

To deal with the usual speed restriction below 10000 ft, we have to abandon the above scenario, because we cannot minimize fuel consumption with respect to speed anymore. If the speed is given (in terms of R), equation (3) still has one degree of freedom, connecting T/W to the flight path angle γ , and we have to solve for a fuel-to-distance-optimal climb strategy in a different way now.

Implementing a 250 KIAS restriction including conversion to true airspeed, we get an altitude-dependent prescribed speed $V_F(h)$. Since air density ρ is also h -dependent, so is the dynamic pressure $\bar{q}(h) = \frac{1}{2}\rho(h)V_F(h)^2$ and the variable $U(h) = \bar{q}(h)S$ connecting the pressure ratio R to the weight W via

$$R(h, W) = \frac{\bar{q}(h)}{\frac{W}{S}} = \frac{\rho(h)V_F^2(h)S}{2W} = \frac{U(h)}{W}.$$

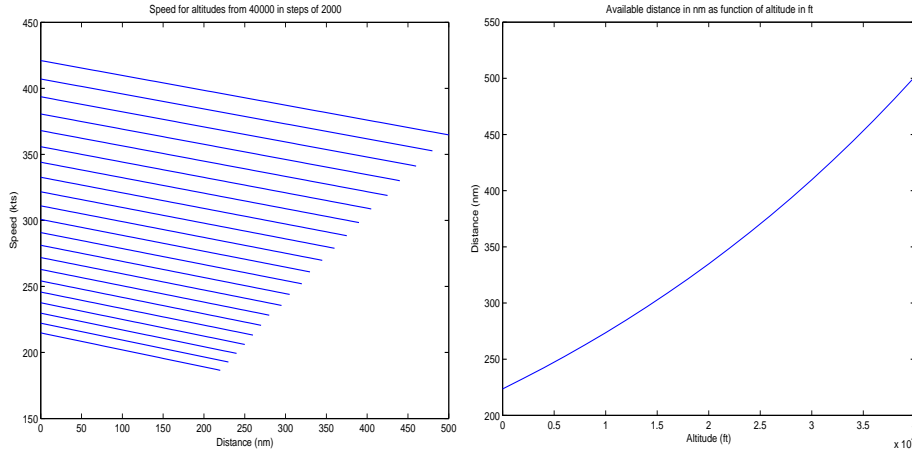


Figure 5: Speed profiles and reachable distances for fuel-optimal flight at constant altitude

Then (3) yields

$$T = C_{D_0}U(h) + \frac{KW^2 \cos^2 \gamma}{U(h)} + W \sin \gamma.$$

Inserting into the fuel consumption integrand, we get

$$-W'(x) = \frac{C(h)}{V_F(h)} \left(\frac{C_{D_0}U(h)}{\cos \gamma} + \frac{KW^2 \cos \gamma}{U(h)} + W \tan \gamma \right)$$

which is a Lagrangian $L(W, h, h') = L(W, u, v)$ and leads to a variational problem with an Euler-Lagrange equation. In contrast to Section 4, the weight is not eliminated, but we simply keep it in the Lagrangian. We only need the Lagrangian for h up to 10000 ft, and then we can fit each h -dependent part with good accuracy by a low-degree polynomial in h . The γ - or $h' = \tan \gamma$ - dependent parts can be differentiated symbolically, as well as the polynomial approximations to the h -dependent parts. We get the ODE system

$$\begin{aligned} h' &= v \\ v' &= \frac{1}{L_{vv}(W, u, v)} (L_u(W, u, v) - L_{vu}(W, u, v)v) \\ W' &= -L(W, u, v) \end{aligned}$$

for the Euler-Lagrange flight paths, under suitable initial or boundary value conditions, and we can roughly repeat Section 4 for the new variational problem. Above, the subscripts denote the partial derivatives.

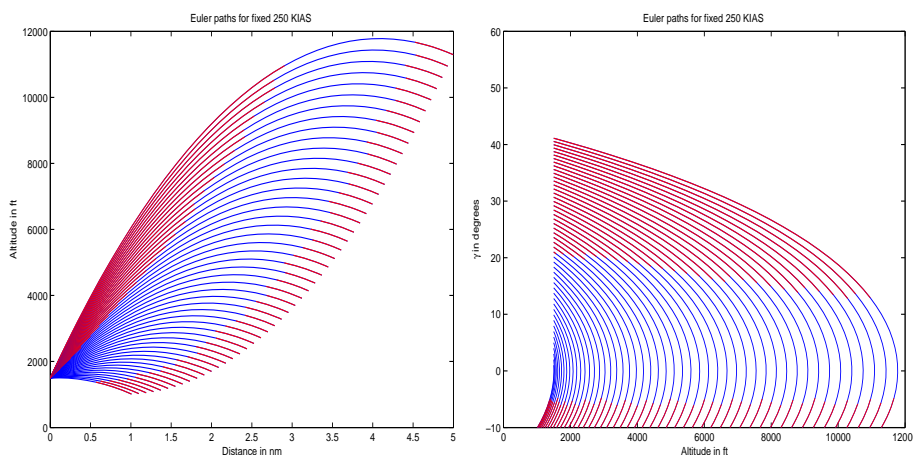


Figure 6: Euler paths for climbing at 250 KIAS, as flight paths and in phase space

For the aircraft model in [7], we get Figure 6 showing trajectories in (x, h) space and in (h, γ) phase space between 1500 and 10000 ft, the red parts violating the thrust restrictions. Like our arguments for FtX speed above 10000 ft, we see that fuel-to-distance optimal trajectories, if they are not violating thrust restrictions, must follow a blue curve. All others must follow the boundaries of the restrictions they violate. For the standard case of climbing to 10000 ft, we have to select a trajectory in phase space that meets $\gamma = 0$ at 10000 ft. There is only one that arrives there at $\gamma = 0$, and it has to be flown from low altitude using maximal admissible continuous thrust, following the red/blue boundary up to a point where thrust is reduced to follow the blue curve up to 10000 ft and $\gamma = 0$. All other climbing trajectories that reach 10000 ft do so at certain positive final angles, and they all use maximal thrust for most of their climb. If thrust and speed are prescribed, the basic equation (3) for quasi-optimal flight is solved for γ , and it is easy to come up with the ODE system for $h(x)$ and $W(x)$.

But these trajectories need 250 KIAS at their start on the red/blue boundary, and this calls for acceleration at the “acceleration” altitude where clean configuration is reached and “*at which the aircraft accelerates towards the initial climb speed*” [1, p. 1245].

7 Acceleration at Fixed Altitude

The final speed of the previous section will be 250 KIAS at 10000 ft, irrespective of the final angle, and we want to continue with an optimal fuel-to-distance flight

path at FtX speed. But this requires a much higher speed at 10000 ft, calling for an acceleration. Another acceleration will be necessary at acceleration altitude after takeoff and before climbing, as we saw in the previous section, because we need 250 KIAS.

For acceleration at fixed altitude, thrust is the only remaining degree of freedom, and we have no quasi-steady flight anymore. The equations now are

$$\begin{aligned}\dot{x} &= V \\ \dot{W} &= -CT \\ \dot{V} &= \frac{g}{W}(T - D) \\ 0 &= L - W,\end{aligned}$$

and we use the last one to eliminate C_L via

$$C_L = 2 \frac{W}{\rho V^2 S}.$$

We plug this with the drag polar into the ODE for speed and get

$$\frac{\dot{V}}{g} = \frac{T}{W} - C_{D_0} R - K/R, \quad R = \frac{\rho V^2 S}{2W}$$

after a few simplifications. Together with $\dot{W} = -CT$ this is a system of two ODEs for W and V with given T . There is nothing to optimize. If we want to go from speed V_0 to speed V_1 , we should rewrite the system as one for x and W in terms of V . Using primes temporarily for derivatives wrt. V , we get the system

$$\begin{aligned}x' &= \frac{V}{\dot{V}} \\ W' &= \frac{\dot{W}}{\dot{V}}\end{aligned}$$

and insert \dot{V} and \dot{W} from above. On the theoretical side, we see that in order to get any acceleration, thrust must satisfy

$$\frac{T}{W} \geq C_{D_0} R + K/R \geq C_{D_0} R_{L/D} + K/R_{L/D} = 2\sqrt{KC_{D_0}},$$

and if thrust is only somewhat larger than the right-hand constant, we can only accelerate from speeds near to $V_{L/D}$, and the acceleration will be only slowly getting better by loss of weight. We note in passing that this argument supports the statement [8] ” *Green dot speed is the one or 2 engine out operating speed in clean configuration; being approximately the best lift-to-drag ratio speed, it provides*

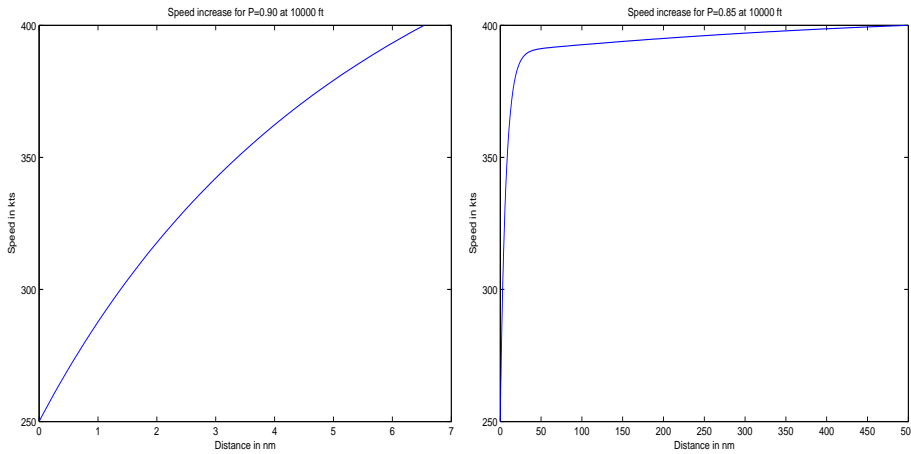


Figure 7: Acceleration for two power settings.

in general the lowest fuel consumption”, because it is the speed of choice for all cases of low thrust, in particular in case of engine failure. But the “lowest fuel consumption” of green dot speed is true only against time, not distance.

Figure 7 shows acceleration of the model aircraft at 10000 ft from 250 to 400 kts as a function of distance in nm. The left-hand plot uses $P = 0.90$ and needs 6.5 nm, while the right-hand plot uses $P = 0.85$ and takes 500 nm and consumes plenty of fuel.

If this is incorporated into a full optimization of fuel consumption of a long-distance flight, one also has to check the consumption in relation to covered distance. Figure 8 shows the speed profile for $P = 0.86$ to 0.98 in steps of 0.01 , and the corresponding fuel consumption, absolutely and in relation to the covered distance. Now a low power setting uses less fuel per mile, but the rate is still much too high compared to flight at high altitude. For a long-distance flight, it is easy to check by simple calculations that it pays off to be able to start a speed-optimal climb quickly, i.e. to accelerate at high power setting. The situation for an acceleration altitude of 1500 ft and acceleration to 250 KIAS is quite similar, but takes at most 2 nm. In Section 8 we take a closer look into how acceleration pays off.

Here is a little detour. The same arguments apply for deceleration at constant altitude and fixed idle thrust, and the same equations work. If started either at a Final Approach Fix at 3000 ft and 250 kts or for a flare over a runway at 10 ft and 150 kts, there is a sharp stalling effect given in Figure 9 This is calculated in clean configuration without flaps, and the crash occurs after roughly 7 or 1.8 nm, respectively. The nice linear speed reduction at the beginning might lure

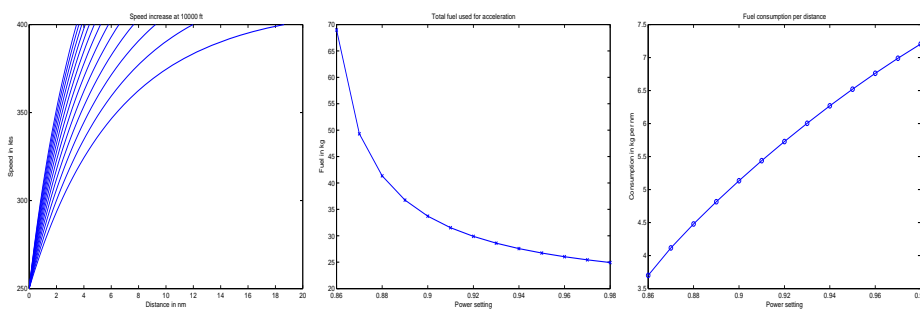


Figure 8: Speed and absolute/relative fuel consumption for acceleration.

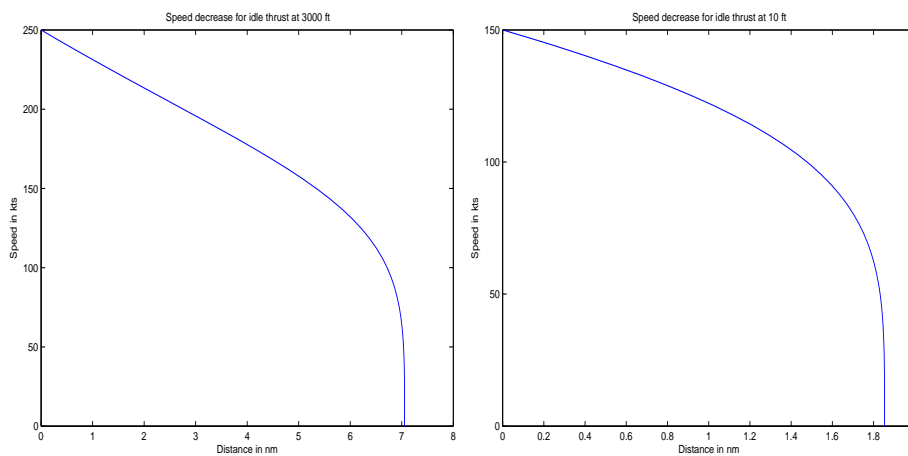


Figure 9: Speed for deceleration at idle thrust and fixed altitude until stall, for 3000 ft and 250 kts (left) and 10 ft and 150 kts (right), the flare situation.

unexperienced pilots into assuming that this decrease goes on, but the speed drop-off is sudden, unexpected, and dramatic.

8 Climb to Prescribed Altitude

We now compare two basic strategies for climbing from 10000 ft to some prescribed high altitude:

1. the *FtX* strategy:
 - (a) accelerate to *FtX* speed at 10000 ft with thrust T_{max} ,
 - (b) do an *FtX* climb with T_{max}
 - (c) stop it in time with an Euler path to arrive at the given altitude.
2. the *LtD* strategy:
 - (a) climb at T_{max} with *LtD* speed, i.e. maximal climb rate,
 - (b) at the final altitude, accelerate at T_{max} to the speed *FtX* will need,
 - (c) then use the optimal *FtX* speed until arriving at the same point and speed as the previous case.

To make the two cases comparable, we have to begin and end at the same altitude and speed. This implies that we have to deal with the horizontal flight in the second case in an optimal way. Since we know that *FtX* speed at constant altitude uses less fuel per distance than *LtD* speed at constant altitude, we have to use *FtX* speed there. We want to see the payoff of the higher speed in the *FtX* case, and evaluate the fuel savings. Besides, we want to check whether acceleration at a higher altitude (case *LtD*) is preferable to acceleration at a lower altitude (case *FtX*). The first case has the advantage of lower air density, but the second has more available thrust and can do the acceleration in much less time. Note that acceleration in the sense of physics is independent of altitude, just an action involving force, mass and speed, but force will depend seriously on altitude here. Another argument for making this comparison is the possibility that using V_{LtD} on a trajectory being too steep for V_{FtX} may be advantageous, because this case lies outside of what was discussed up to this point, since we focused on trajectories that allow V_{FtX} speed.

Figure 10 shows the results for the model aircraft climbing from 10000 to about 25000 ft. All curves have the above three consecutive phases. The flight paths (top left) show the *LtD* case as the upper curve, with the steep climb, the acceleration to *FtX* and the horizontal *FtX* flight. The lower *FtX* path first accelerates, then

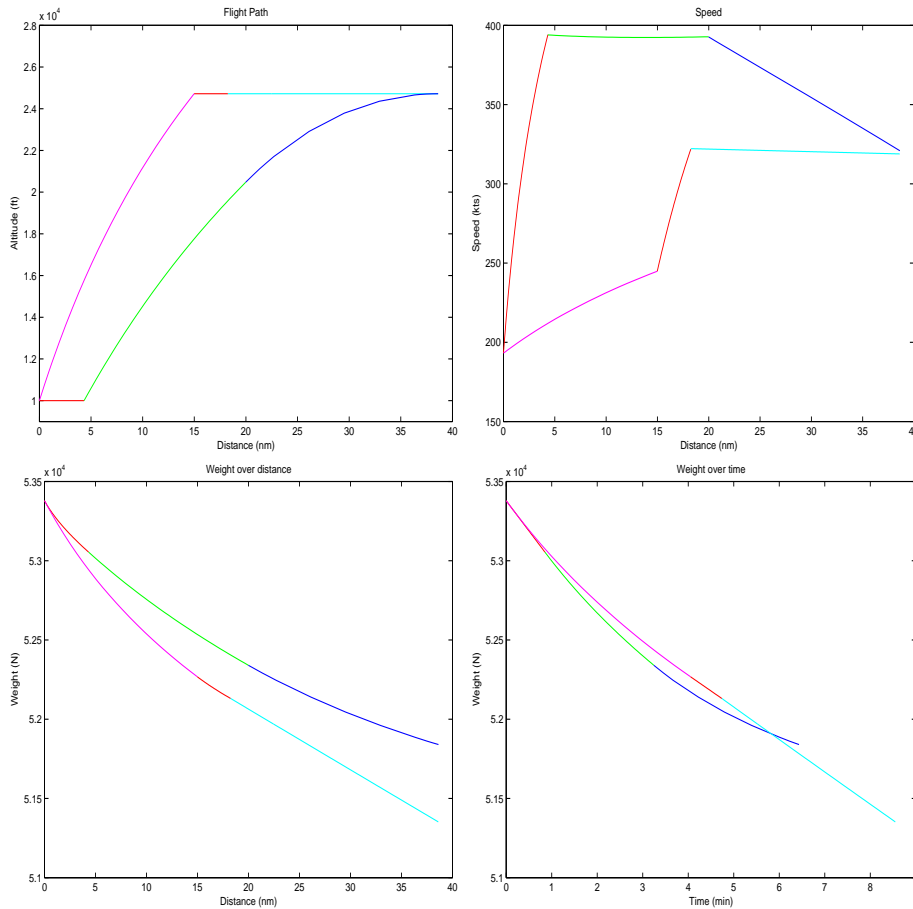


Figure 10: Flight path, speed, and weight for a climb from 10000 ft to 25000 ft

climbs at FtX speed, and then goes into an Euler path. The speed plot (top right) uses the same colors and clearly shows the serious differences in speed. Below, we plotted the weight as a function of distance (left) and time (right). Over distance, the FtX case is *always* superior to the LtD case, which is clear by definition if used on the same flight path, but here the flight paths are considerably different. With respect to time, LtD speed uses less fuel than FtX if used on the same flight path, but the FtX flight path is again the better choice, leading after about 4 minutes to less consumption per time than V_{LtD} on its flight path. In addition, the FtX case covers more distance due to higher speed, and it reaches the common goal about two minutes earlier than the LtD case. The fuel consumption is 330 kg in the LtD case and 157 kg in the FtX case, a serious savings in favor of V_{FtX} and its flight path.

This example shows that the FtX strategy is superior to LtD not only in cruise, but even more in climb. And, though it uses less fuel per distance, an FtX flight will arrive earlier than a LtD flight, due to the larger groundspeed both in climb and cruise.

9 Flight Level Change in Cruise

We now consider the practical situation that a long-distance high-altitude cruise under Air Traffic Control is a sequence of level flights with various short-term flight-level changes. These are short-term changes of γ , and it is debatable whether they should be considered as quasi-steady flight. We know from Section 5 that such a flight is never fuel-to-distance-optimal, but each level section should apply the V_{FtX} speed given by (7). This means that all level flight sections in cruise use the same R_{FtX} and T/W ratio, no matter what the flight level or the propulsion model is. Only the drag polar is relevant.

The V_{FtX} speed at $\gamma = 0$ then is a function of weight and altitude alone, and flight level changes should comply with this, i.e. the speed should still vary smoothly, while γ and thrust may change rapidly. We shall deal with this by keeping the flight level change as quasi-steady flight, except for the beginning and the end, where we allow an instantaneous and simultaneous change of γ and thrust.

The idea is to keep the quasi-steady flight equation (3) and the R_{FtX} equation (7) valid at all times. Then a jump in γ must be counteracted by a jump in thrust, one in the beginning and one in the end of the flight level change. These instants are not quasi-steady, but the rest is.

Consider a climb from altitude h_0 to altitude h_1 . When flying at V_{FtX} at h_0 at maximal thrust $T_{max}(h_0)$, the flight level change is impossible. Otherwise, the quasi-steady flight equation (3) at time t_0 and $\gamma = 0$ is

$$\frac{T_0}{W_0} = C_{D_0} R_{FtX} + \frac{K}{R_{FtX}}, \quad T_0 < T_{max}(h_0), \quad (10)$$

and we apply maximal thrust and go over to

$$\frac{T_{max}(h_0)}{W_0} = C_{D_0} R_{FtX} + \frac{K}{R_{FtX}} \cos^2 \gamma_0 + \sin \gamma_0$$

defining a unique climb angle γ_0 satisfying

$$2K \sin \gamma_0 = R_{FtX} - \sqrt{R_{FtX}^2 - 4K \frac{T_{max}(h_0)}{W_0} R_{FtX} + 4KC_{D_0} R_{FtX}^2 + 4K^2}. \quad (11)$$

We could keep this angle for the climb, but we might reach the thrust limit if we do so. Therefore we prefer to satisfy

$$\frac{T_{max}(h)}{W(h)} = C_{D_0} R_{FtX} + \frac{K}{R_{FtX}} \cos^2 \gamma(h) + \sin \gamma(h)$$

at each altitude using

$$K \sin \gamma(h) = R_{FtX} - \sqrt{R_{FtX}^2 - 4K \frac{T_{max}(h)}{W(h)} R_{FtX} + 4K C_{D_0} R_{FtX}^2 + 4K^2}.$$

This is put into an ODE system for h and W with γ as an intermediate variable, namely

$$\begin{aligned} h' &= \tan \gamma(h) \\ W' &= -\frac{C(h) T_{max}(h)}{V_{FtX}(h, W) \cos \gamma(h)}. \end{aligned}$$

The result is a climb with constant R_{FtX} that keeps V_{FtX} of (7) at all times and thus starts and ends with the correct speed for FtX level flight. For descent, the same procedure is used, but idle thrust is inserted. If the altitude change is small, the solution is close to using the fixed climb/descent angle γ_0 of (11). At the end of the flight-level change at altitude h_1 , the final speed $V_{FtX}(h_1, W_1)$ is the starting speed of the next level flight, and the thrust has to be decreased instantaneously to T_1 in order to keep the ratio

$$\frac{T_0}{W_0} = \frac{T_1}{W_1}$$

from (10).

We omit plots for our standard aircraft model, because they all show that the crude simplification

$$\frac{h_1 - h_0}{x_1 - x_0} \approx \gamma_0 \approx \frac{T - T_0}{W_0}$$

holds for small altitude changes between level flights, where the thrust T is either T_{max} or T_{idle} . Thus in (x, h) space the transition is very close to linear with the roughly constant climb angle given above.

But we have to ask whether climbing at maximal thrust is fuel-to-distance optimal against all other choices of thrust. If we insert the above approximation into the fuel consumption with respect to the distance and just keep the thrust varying, we get

$$\int_{x_0}^{x_1} \frac{CT}{V \cos \gamma} dx \approx W_0(h_1 - h_0) + T_0(x_1 - x_0)$$

up to a factor, and thus we should minimize the climb angle if we relate consumption to distance. For descent, this leads to taking T_{idle} and is easy to obey, but for climb the fuel-optimal solutions cannot be taken because they take too long. Consequently, pilots are advised to perform the climb at smallest rate allowed by ATC.

10 Flight Phases for Optimal Fuel Use

As long a Air Traffic Control does not interfere, we now see that a long fuel-to-distance optimal flight should have the following phases:

1. Takeoff to clean configuration and acceleration altitude,
2. accelerate there to 250 KIAS at maximal admissible continuous thrust, using Section 7,
3. climb at maximal admissible continuous thrust, keeping 250 KIAS and following the fuel-to-distance-optimal angle selection strategy of Section 6, and continuing with
4. a solution of the variational problem given there to end at precisely 10000 ft,
5. accelerate at 10000 ft until the required FtX speed for the climb is reached, using Section 7 again,
6. perform an FtX climb/cruise following Sections 4 and 5 at maximal continuous admissible thrust until shortly before the top-of-descent point, leaving that climb for
7. an Euler path satisfying the variational problem of Section 4 until thrust is idle,
8. do a continuous descent at idle thrust down to the Final Approach Fix.

To arrive at the right distance and altitude, the time for starting phase 7 needs to be varied, like in Figure 4.

If ATC requires horizontal flight phases and correspondent flight-level changes, step 6 is followed by

- 6a. an Euler path satisfying the variational problem of Section 4 to reach the prescribed altitude,

- 6b. using Section 5 for FtX speed at level flight, and
- 6c. flight path changes following Section 9,

but the flight will not be fuel-optimal with respect to distance. Various examples show that a continuous descent from high altitude ends up at speeds below 250 KIAS at 10000 ft, and deceleration is not needed.

For short-distance flights, the situation is different. Very short flights may follow Figure 6 and can stay roughly below 10000 ft, but might go off the red/blue boundary early, follow a blue trajectory over a top altitude downward until reaching the lower red/blue boundary, i.e. doing a continuous descent at idle thrust while moving to the left in phase space.

Medium-distance flights perform the first three steps completely and then continue by paths in in Figure 2. If they do not reach the upper red/blue boundary in phase space, they follow a blue curve downward and then end with continuous descent at idle thrust. All longer flights run along the upper red/blue boundary to the right and leave at some point to follow a blue curve downward.

Altogether, all of these flight paths follow the above steps for long-haul flights up to a certain point where they take a “shortcut” from the long-distance flight pattern. Like in our treatment of the flight level change, we keep the speed continuous and allow simultaneous jumps in T and γ that allow to continue with an Euler piece of Section 4. Thus we can plot them all in one figure, the final altitude and distance depending on when the shortcut is taken.

Figure 11 shows the flight paths, a close-up, and the speed assignment for short- and medium distance flights. The acceleration phases at 1500 ft and 10000 ft are in cyan (the first being too short to be well visible), the 250 KIAS climb in red, followed by a short Euler piece for the variational problem of Section 6 in magenta, and the second acceleration at 10000 ft, in cyan again. From this basic flight plan, blue Euler pieces of Section 4 emanate, followed by continuous descent by idle thrust plotted in green. All flights end at 3000 ft at reasonable speeds.

If long-distance flights are included, the basic behavior is like in Figure 4, extending Figure 11 to the right, but we add a phase space plot in Figure 12 that agrees well with Figure 2. If we take the fuel consumption of each full flight and divide by the distance covered, we get the right-hand plot, showing the relative fuel efficiency of long-distance flights over short-distance flights.

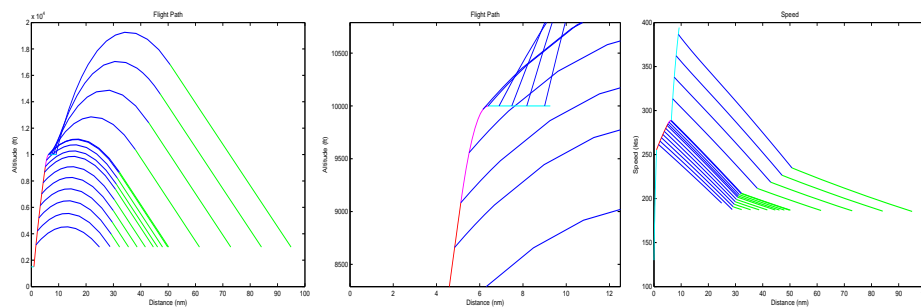


Figure 11: Flight paths for short- and medium distance, in (x, h) space, a close-up of the transition, and speed, all as functions of distance.

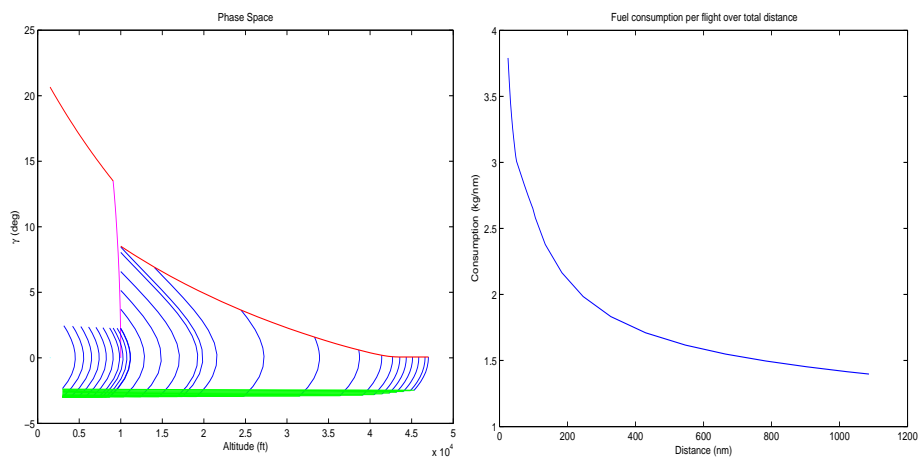


Figure 12: Flight paths in phase space, and consumption

11 Summary and Open Problems

For total fuel consumption over a flight, the choice of V_{FIX} speed is clearly advantageous, since it can be expected to save more than 14% fuel and will also result in earlier arrival than the optimal lift-to-drag or fuel-to-time speed. It buys this advantage by larger groundspeed, at the expense of two rather short additional acceleration phases. Optimal flight paths with V_{FIX} speed assignments either use maximal or minimal thrust, or follow a flight path solving the Euler equation of a variational problem. There are two of these: one for unrestricted speed and one for the 250 KIAS restriction below 10000 ft. Full flight plans can be assembled from the various pieces described in the paper.

The basic restriction here is that we strictly consider quasi-steady flight, with instantaneous exceptions where thrust and flight path angle are varied abruptly. Also, the numerical examples are currently confined to the Small Business Jet of [7] with its turbojet engines and simplified propulsion models. However, most of the results are general enough to be easy to adapt for other aircraft and engine characteristics.

References

- [1] Airbus. *Airbus A 380 Flight Crew Operating Manual*. Airbus S.A.S Customer Services Directorate, 31707 Blagnac, France, 2011. Reference: KAL A 380 Fleet FCOM, Issue Date: 03 Nov. 2011.
- [2] J.W. Burrows. Fuel optimal trajectory computation. *Journal of Aircraft*, 19:324–329, 1982.
- [3] A. Franco and D. Rivas. Analysis of optimal aircraft cruise with fixed arrival time including wind effects. *Aerospace Science and Technology*, 32:212–222, 2014.
- [4] A. Franco, D. Rivas, and A. Valenzuela. Minimum-fuel cruise at constant altitude with fixed arrival time. *Journal of Guidance, Control, and Dynamics*, 33:280–285, 2010.
- [5] J. García-Heras, M. Soler, and F.J. Sáez. Collocation methods to minimum-fuel trajectory problems with required time of arrival in ATM. *Journal of Aerospace Information Systems*, 13:243–265, 2016.
- [6] A. Gardi, R. Sabatini, and S. Ramasamy. Multi-objective optimisation of aircraft flight trajectories in the ATM and avionics context. *Progress in Aerospace Sciences*, 83:1–36, 2016.

- [7] D.G. Hull. *Fundamentals of Airplane Flight Mechanics*. Springer, 2007.
- [8] O. Husse. Best practices for fuel economy. Lecture Slides, ICAO Operational Measures Workshop / Montreal, 20/21 September 2006.
- [9] W. Maazoun. *Conception et analyse d'un système d'optimisation de plans de vol pour les avions*. PhD thesis, École Polytechnique de Montréal, 2015.
- [10] S.G. Park and J.-P. Clarke. Optimal control based vertical trajectory determination for continuous descent arrival procedures. *Journal of Aircraft*, 52:1469–1480, 2015.
- [11] W. F. Phillips. *Mechanics of Flight*. John Wiley & Sons, 2010. Second Edition.
- [12] B.L. Pierson and S.Y. Ong. Minimum-fuel aircraft transition trajectories. *Mathematical and Computer Modelling*, 12:925–934, 1989.
- [13] A. Saucier, W. Maazoun, and F. Soumis. Optimal speed-profile determination for aircraft trajectories. *Aerospace Science and Technology*, 2017. In Press.
- [14] R.F. Stengel. Lecture slides for aircraft flight dynamics. <https://www.princeton.edu/~stengel/MAE331Lectures.html>, 2014.
- [15] A. Valenzuela and D. Rivas. Optimization of aircraft cruise procedures using discrete trajectory patterns. *Journal of Aircraft*, 51:1632–1640, 2014.